Optical Microscopic Study on the Morphologies of Isotactic Polypropylene Induced by Its Homogeneity Fibers

Huihui Li,† Shidong Jiang, Jijun Wang, Dujin Wang, and Shouke Yan*

State Key Laboratory of Polymer Physics and Chemistry, Joint Laboratory of Polymer Science and Materials, Institute of Chemistry, Chinese Academy of Sciences, Beijing 100080, P. R. China

Received January 20, 2003; Revised Manuscript Received February 25, 2003

ABSTRACT: Through introducing the iPP fibers into their supercooled homogeneity matrices, the homogeneity fiber/matrix composites of iPP have been prepared, and the resulting supermolecular structures of iPP matrices induced by their homogeneity fibers as a function of introduction temperature were studied by means of optical microscopy. The results show that the supermolecular structures of iPP matrices induced by their homogeneity fibers can be ascribed to the transcrystallization of iPP triggered by strong heterogeneous nucleation rather than the shear stress produced by fiber introduction. The morphological features demonstrate that the interfacial transcrystalline iPP is composed of purely α-form if the fibers were introduced at 138 °C. With increase of fiber introduction temperature, an increasing content of *β*-iPP surrounding the iPP fibers has been observed. A transcrystallization layer of mainly *β*-modification iPP can be obtained when the fiber introduction temperature was set at 173 °C. This is associated with melting or at least partial melting of the iPP fibers. The formation of rich α-iPP transcrystallization layers at an even higher fiber introduction temperature, e.g., 178 °C, further demonstrates that the melting state of the iPP fibers plays an important role in generating the *β*-iPP.

Introduction

Isotactic polypropylene (iPP) is one of the semicrystalline polymers exhibiting pronounced polymorphic crystalline modifications designated as monoclinic α-form, trigonal (or frequently hexagonal) *β*-form, and orthorhombic *γ*-form.[1−5] It was well documented that the monoclinic α-form, commonly produced by melt crystallization, is its thermodynamically most stable crystalline form. Since the nucleation of metastable *β*-form occurs much more rarely in bulk crystallization than that of the predominant α-modification, it can only be obtained through special crystallization procedures, such as in a thermal gradient,[6] shearing or elongation of the melt during crystallization,[7] with special nucleating agents during bulk crystallization,[8,9] and so on. Among them, bulk crystallization with *β*-form nucleating agents is generally used for generating *β*-form iPP, while shear stress-induced *β*-form iPP column structures are most frequently encountered in the fiber/iPP composites.[10−14]

In the past few decades, much attention has been paid to the composite systems composed of iPP matrix and a variety of inorganic or polymer fibers, such as carbon, glass, Kevlar, PET, nylon, and PTFE fibers.[15−19] It was found that transcrystalline morphologies of iPP in the vicinity of the fibers could be produced as long as the used fibers exhibit strong heterogeneous nucleation ability toward iPP. However, column structures surrounding the fibers were always the observed morphologies of iPP, regardless of their nucleation abilities, whenever the fibers were pulled during the crystallization process of iPP. For example, the unsized glass fiber, which shows no nucleation capability toward iPP in static melt, can induce column structures of iPP by pulling the fiber during crystallization of iPP matrix.[11] To distinguish the column structure generated by fiber pulling from the transcrystalline structure triggered by surface-induced heterogeneous nucleation, Varga et al.[13] have defined the shear-induced column structure as "cylindrite". It was reported that the supermolecular structures of iPP in the shear-induced cylindrites are different from those in the transcrystalline zone. When crystallizing from static melt, the monoclinic α-form was the observed morphology of iPP in the vicinity of the fibers as well as in the areas of bulk crystallization. In the shear-induced crystallization of iPP through fiber pulling, cylindrites with *β*-iPP as a rich phase were, however, usually produced. The content of the *β*-iPP in the cylindrites depends remarkably on the crystallization and fiber-pulling temperatures.

Recently, there is an increasing interest in the field of self-reinforced homogeneity polymer composites due to both their ideal recyclability and expected improvement of interfacial bonding.[20,21] A number of articles have been seen in the literature. However, most of the work focused on the single-polymer composite of polyethylene prepared via specific processing. The only reported work dealing with the iPP homogeneity composite was described by Loos et al.[22] In their work, the homogeneity composite of iPP was prepared by compression-molding the nonoriented iPP thin films, ca. 80 *μ*m in thickness, together with the highly oriented iPP fibers, which were end-fixed on a glass slide, at 170 °C for 5 min. It was confirmed that the used procedure has molten only the iPP matrix material but not the constrained fibers, so that the single-polymer composite of iPP was prepared. Morphological studies on thus-prepared homogeneity composites via optical and scanning electron microscopy illustrate the formation of α-form iPP transcrystalline layers in the vicinity of iPP fibers. Unfortunately, a more detailed morphological study on the thus-prepared homogeneity composites is difficult due to the similar melting behaviors of the iPP matrix and fibers.

† Ph.D. candidates of the Chinese Academy of Sciences.

* To whom all correspondence should be addressed: e-mail skyan@iccas.ac.cn, Tel 0086-10-82618476, Fax 0086-10-62559373.

10.1021/ma034062w CCC: $25.00
Published on Web 03/27/2003

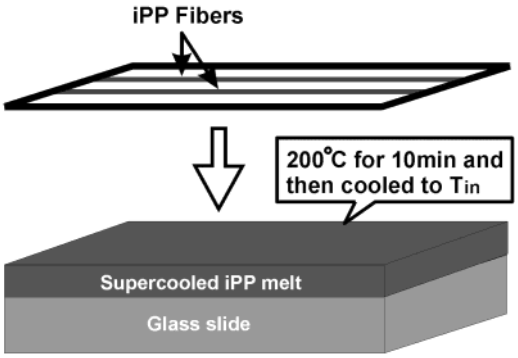

Figure 1. A sketch shows the sample preparation procedure.

In this work, the fact that polymer melts can only crystallize under supercoolings was utilized, and homogeneity fiber/matrix composites of iPP were prepared by introducing the high-performance fibers into its supercooled melts. With this procedure, the morphologies of the resulting composites as a function of fiber introduction temperature (T_{in}) were studied in detail by means of optical microscopy. The purpose of this paper is to present some detailed experimental results about the effect of T_{in} on the polymorphic behavior of iPP in the fiber/matrix interfacial layers.

Experimental Section

The matrix polymer used in this work was commercial grade isotactic polypropylene (iPP), GB-2401, with melt flow index of 2.5 g/10 min, $M_w \approx 437\,900$, and melting temperature of 170 °C, produced by Yanshan Petroleum and Chemical Corp., China. The granular iPP materials were used without any further treatment. The iPP fibers were produced with homemade melt-spinning device. The spinning temperature was 200−240 °C. The resulting iPP fibers were then subjected to a cold-draw procedure at 110 °C with a draw ratio of 6. The material used for fiber spinning is chemically degraded iPP GB-2401 a melt flow index of 15 g/10 min, $M_w \approx 245\,100$, $M_n \approx 73\,600$, and melting temperature of 170 °C. The average diameter of thus-prepared iPP fibers is ca. 20 μm. To remove the sizing agents on the fiber surface, the fibers were treated for 4 h with refluxing acetone and then dried in a vacuum oven at 40 °C for 5 h. Thin iPP films, 40−50 μm in thickness, were prepared by compression-molding the iPP granules at 200 °C with a pressure of 75 kg/cm^2. The iPP fiber/matrix homogeneity composites were produced by a procedure as shown in Figure 1. The iPP matrix thin film was first heated to 200 °C for 10 min to erase possible effects of thermal history of the sample on the subsequent crystallization and then moved to a preheated heat plate, where the iPP matrix was kept in the molten state or supercooled molten state at the moment of fiber introduction. As the iPP molten or supercooled molten thin layer reached an equilibrium at the desired temperature, homogeneity iPP fibers tightly fixed on a metal frame (as shown in Figure 1, upper part) were introduced into the iPP matrix. The fiber introduction temperatures used in this study were 138, 160, 168, 173, and 178 °C. After introduction of the fibers, the prepared iPP fiber/matrix composites were subsequently moved quickly to another heat plate at 138 °C, and isothermal crystallization of the iPP supercooled melts was allowed for 6 h.

For optical microscopy observation, an Olympus BH-2 optical microscope was used in this study. All optical micrographs presented in this paper were taken under cross-polarized light.

Results

Figure 2 shows the optical micrographs of an iPP fiber/matrix homogeneity composite, which was prepared by introducing the iPP fibers into their supercooled homogeneity matrix at 138 °C and subsequently keeping the sample at this temperature for 6 h. From Figure 2, the morphological difference between iPP in the vicinity of its homogeneity fibers and those in the areas away from the fibers clearly indicates that the iPP matrix was indeed kept in its supercooled molten state at the moment of fiber introduction. Here the sample shows two different morphologies, i.e., the column layers of iPP matrix surrounding its homogeneity fibers and the spherulitic structures of iPP matrix away from the fibers. Birefringence measurements indicate an optical negative character of the interface layers surrounding the iPP fibers and the matrix spherulites. Melting test demonstrates the formation of monoclinic α-modification in both areas with spherulitic and column structures. This has a close resemblance with that obtained by Loos et al.,[22] where also only crystalline α-phase of iPP was created. Moreover, the density of the iPP nuclei generated on its own fiber surface is too high to resolve each individual one on an optical level, even on the enlarged optical micrograph (Figure 2b).

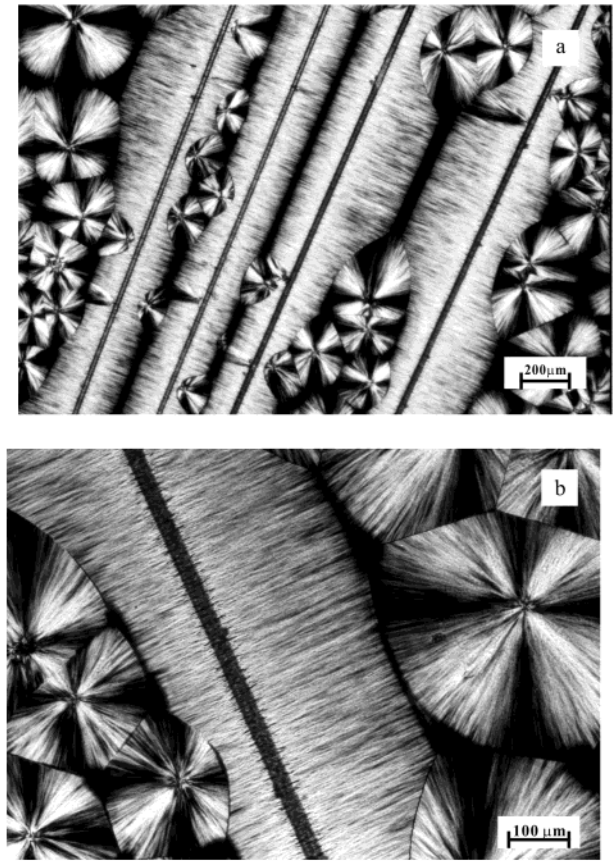

Figure 2. Optical micrographs illustrate the morphologies of an iPP fiber/matrix homogeneity composite. The fiber introduction temperature was 138 °C.

Figure 3 shows the optical micrographs of the iPP homogeneity composites prepared by introducing the iPP fibers into their supercooled homogeneity matrices at 160 °C and subsequently moved to another heat plate at 138 °C for a 6 h isothermal crystallization. The difference between the samples shown in Figure 3a,b is that the fibers in the case of Figure 3a were end-fixed throughout the sample preparation process, whereas the ends of fibers in Figure 3b were released after they were introduced into the supercooled iPP matrix. Different sample preparation processes result in different appear-

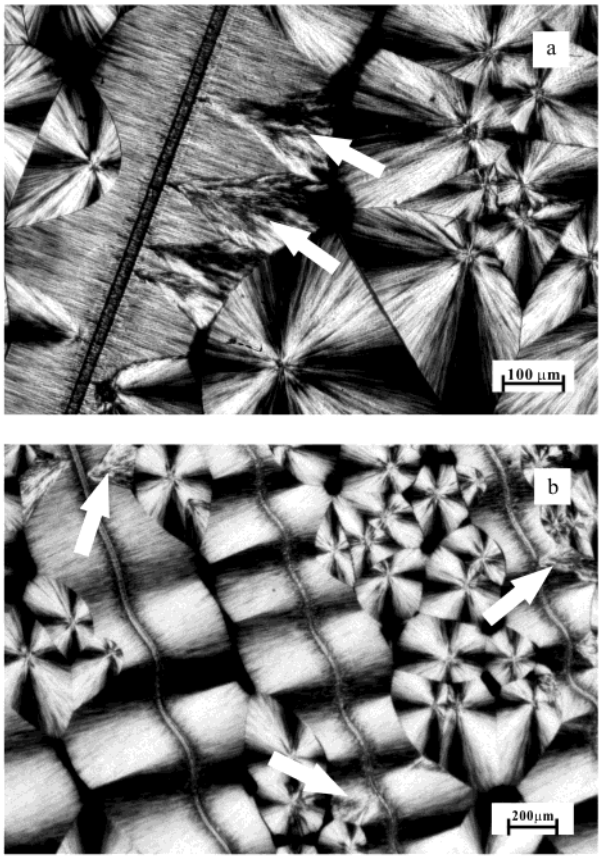

Figure 3. Optical micrographs show the morphologies of the iPP fiber/matrix homogeneity composites. The fiber introduction temperature was 160 °C. The white arrows in the picture indicate the resulted β-iPP. (a) IPP fiber was end fixed during sample preparation. (b) The ends of the iPP fibers were released immediately after introduction of them.

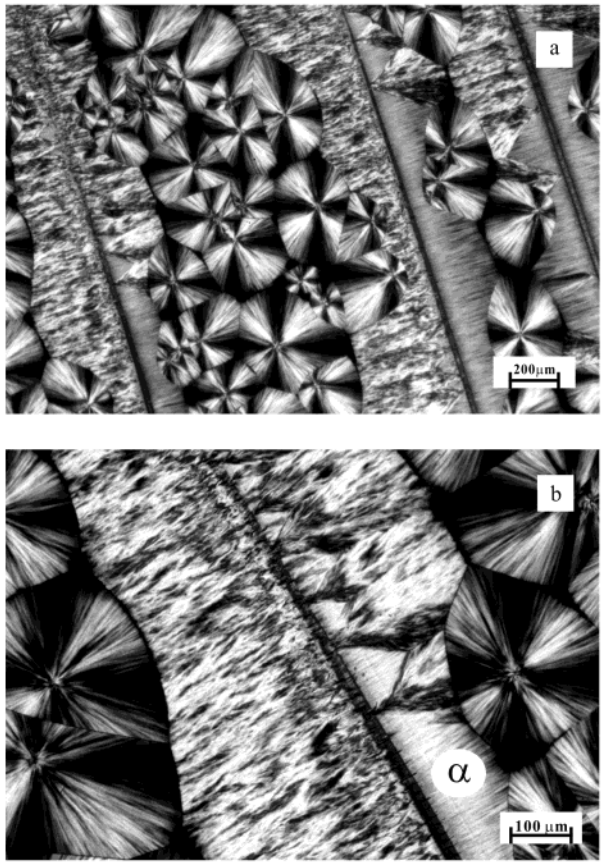

Figure 4. Optical micrographs represent the morphological features of an iPP fiber/matrix homogeneity composite. The "α" in the picture indicates the transcrystalline α-iPP. The fiber introduction temperature was set at 168 °C.

ance of the iPP fibers in Figure 3a,b. The end-released fibers in Figure 3b are evidently bent, while the end-fixed one in Figure 3a is tightly extended. The bending of the iPP fibers in Figure 3b may result from relaxation creepage of them. From Figure 3, it is clear that the resulting spherulitic structures are similar to those presented in Figure 2. Namely, crystalline α-iPP is the observed morphologies in the areas away from the iPP fibers. This is not surprising since the crystallization condition of the iPP was exactly the same for both cases. The supermolecular structures in the interface layers surrounding the iPP fibers are somewhat different from those shown in Figure 2. Even though the α-iPP is still the predominant morphology of the surrounding column layers, there exist several fan-shaped structures sporadically inlaid in the α-iPP column layers, as indicated by white arrows in the pictures. These fan-shaped structures are colorful even without using the λ plate and exhibit very strong negative birefringence. Moreover, they can be molten at about 158 °C. All these are characteristic natures of the β-form iPP and indicate the formation of some crystalline β-iPP. Taking the fact that the same crystallization condition was used for all cases into account, the morphological change is evidently attributed to the enhancement of the fiber introduction temperature. To confirm this conclusion, the fiber introduction temperature was further increased to 168 °C. As illustrated in Figure 4a, now an increasing content of the crystalline β-iPP surrounding the iPP fibers has been seen, while the morphologies in the areas not affected by the iPP fibers remain unchanged. This confirms that increase of fiber introduction temperature is in favor of the formation of β-iPP.

It should be pointed out that the β-iPP crystals are not uniformly arranged along the fibers. From Figure 4a, it can be clearly seen that the fiber on the left side of the picture has mainly initiated the crystallization of iPP matrix in its β-form, whereas the fiber on the right side of the picture is predominantly surrounded by the crystalline α-iPP. The fiber on the middle of the picture is of particular interesting since different supermolecular structures of iPP matrix are generated on different sides of the same iPP fiber, i.e., the α- and β-iPP on the right and left sides of the same iPP fiber, respectively. Through careful observation, it can be found that there exist different responses of the iPP fibers in different areas. The fibers in the areas where β-iPP crystals are generated seem to be molten (see upper left corner of Figure 4a). Also, the fiber located at the middle of the picture becomes thinner and thinner from its bottom to top ends. The melting phenomenon can be more clearly seen from the magnified optical micrograph. As illustrated in Figure 4b, there is a clear boundary line between the iPP fiber and the induced crystalline α-iPP (as indicated by an α). On the contrary, in the top area of the picture with crystalline β-iPP, the iPP fiber can hardly be distinguished from the iPP matrix. The different melting behaviors of the iPP fibers may be associated with either the different local thermal conditions of the sample or the different local qualities of the fibers. In any case, the above-observed phenomenon implies that melting or at least partial melting of

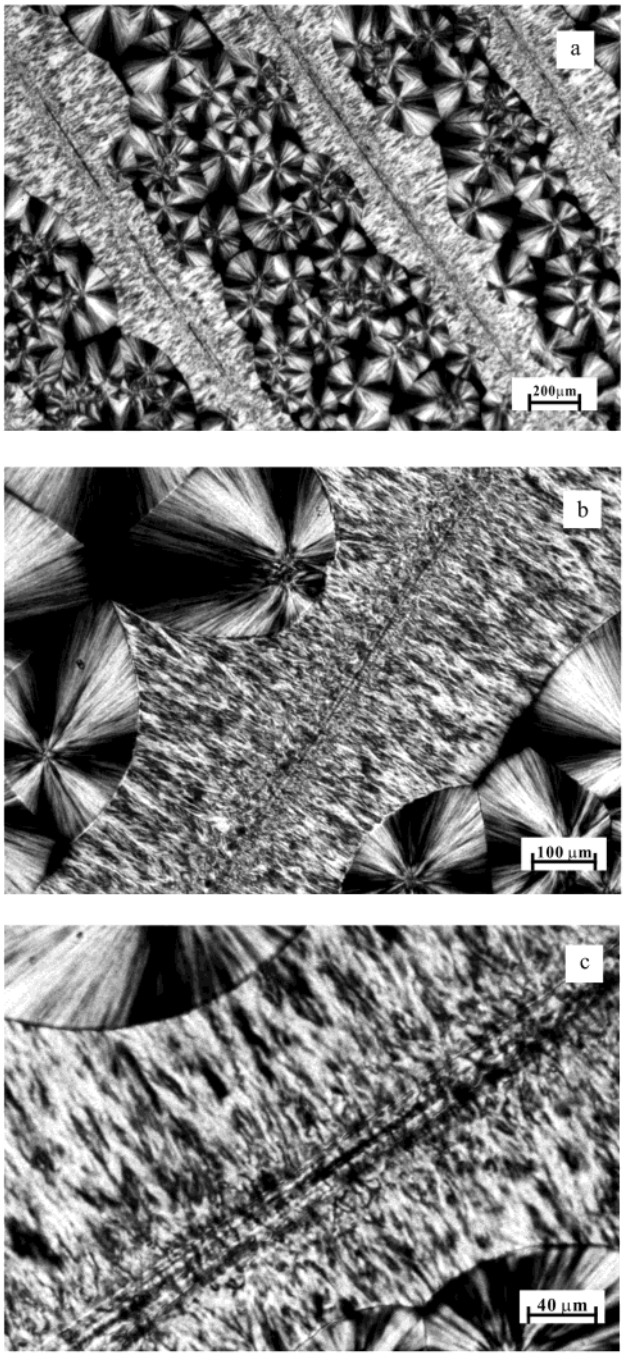

Figure 5. Optical micrographs show the morphologies of an iPP fiber/matrix homogeneity composite. The fiber introduction temperature was 173 °C.

the iPP fiber is in favor of the formation of β-iPP in the fiber/matrix interfacial layer. Therefore, because of either different thermal conductivity of the sample or uneven thermal stability of the fibers, different supermolecular structures have been produced in the same sample, even with the same fiber.

To check the effect of fiber melting on the formation of β-iPP, the fiber introduction temperature was elevated to 173 °C, which is 3 deg above the experimental melting temperature of the used iPP fibers. As presented in Figure 5, the disappearance of the obvious boundary lines between the fibers and the iPP matrix indicates that at present condition all of the fibers have been molten, or at least to some extent. After isothermally crystallized at 138 °C for 6 h, the induced

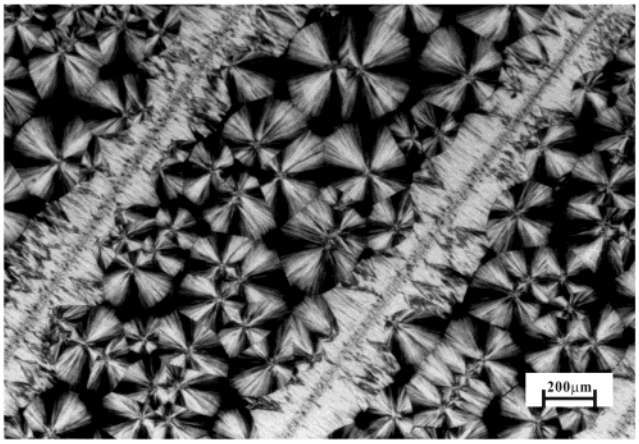

Figure 6. Optical micrograph shows the morphologies of an iPP fiber/matrix homogeneity composite. The fiber introduction temperature was 178 °C.

interface layers are composed of fully crystalline β-modification iPP with very strong birefringence. This unambiguously confirms that melting or surface partial melting of the iPP fiber is the reason for the formation β-iPP.

Figure 6 shows an optical micrograph taken on a sample, which was prepared by introducing the iPP fibers into its homogeneity matrix at an even higher temperature, e.g., 178 °C, and subsequently crystallized isothermally at 138 °C for 6 h. In this particular case, even though the iPP fibers are clearly molten, they remain active for initiating the oriented crystallization of the iPP matrix. But instead of the β-iPP, the interfacial layer consists mainly of α-iPP with some β-iPP dispersed in it. This indicates that the high-temperature melting of iPP fibers has inhibited the formation of β-iPP.

Discussion

According to the above-observed morphological features, two aspects, i.e., (i) the ascription of the column structure surrounding the fibers and (ii) the origin for formation of β-iPP, can be discussed here. First of all, it should be pointed out that, with present sample preparation procedure, some shearing of the molten iPP matrix layer, which is in contact with the iPP fiber, is expected. If the column structures of iPP are created by the expected shear stress, they should be appointed to the crystalline cylindric layers according to Varga's definition.[13] Otherwise, they should be referred to the well-known transcrystallization triggered by strong surface induced heterogeneous nucleation and subsequent spatial confined crystal growth. Varga and Karger-Kocsis[11−14,28,29] have studied the influence of shearing on the morphologies of iPP in the composites made of inorganic fibers and iPP matrix in details. They reported that the existence of shear stress produced by fiber pulling promotes the formation of cylindritic structures of β-iPP. The formation of β-iPP supermolecular structure in sheared composites is not affected by the nucleation ability of the fibers used. They further concluded that the formation of iPP β-modification is limited in a temperature interval with a lower ($T_{\alpha\beta} \approx$ 100 °C) and an upper ($T_{\beta\alpha} \approx 140$ °C) threshold to meet the kinetic requirement of $G_\beta > G_\alpha$, where G_β and G_α represent the crystal growth rate of β- and α-iPP, respectively. The content of the iPP β-modification is

highest when crystallization temperature (T_c) and fiber pulling temperature (T_{pull}) are closely matched within this temperature range, i.e., $T_{\alpha\beta} < T_c \approx T_{pull} < T_{\beta\alpha}$. If the T_{pull} is over $T_{\beta\alpha}$, the proportion of the iPP β-modification decreases or even diminishes irrespective of the isothermal crystallization temperature. The threshold, at which the shear-induced crystallization of iPP disappears, was reported as 170 °C by Wu et al.[29] and 190−195 °C by Varga et al.[28] On the basis of the above discussion, if the shear stress caused by fiber introduction in the present case plays a vital role in iPP crystallization, cylindrites of iPP β-modification should be observed instead of its purely α-counterpart in the case of Figure 2, since $T_c = T_{in} = 138$ °C is well within the aforementioned temperature range. The experimental results are, however, on the contrary. This clearly indicates that the expected shear stress makes no detectable contribution to the crystallization of the iPP matrix. This may be associated with the following: (i) the shear direction in the present experimental procedure, vertical to fiber axis direction, is different from that produced by fiber pulling (along the fiber axis); (ii) restricted by the film thickness of the matrix (40−50 μm), the shearing produced in the present experimental procedure is not sufficient enough to give rise detectable effect on the crystallization behavior of the iPP matrix. On the other hand, the increment of β-iPP with the increase of the fiber introduction temperature is also in contradiction to Karger-Kocsis's conclusion that the β-iPP content decreases with the increase of the fiber pulling temperature. All of these experimental results clearly indicate that the column structures of iPP in the vicinity of its homogeneity fibers are accounted for by the well-known transcrystallization resulted from strong surface-induced heterogeneous nucleation and subsequent spatial confined crystal growth. This reveals conspicuously a high nucleation efficiency of iPP fiber toward its homogeneity matrix. As in the case of polyethylene fiber reinforced polyethylene composites,[23−25] the strong nucleation ability of iPP fiber toward its own matrix may be related to the homoepitaxial crystallization of the iPP matrix on its own fiber surface with (i) exact same chemical composition, (ii) perfect lattice matching, and (iii) better surface wettability.

Second, as already concluded in the last paragraph that the column structures surrounding the iPP fibers are not generated by the shear stress exerted by fiber introduction, the origin of the formation of β-iPP in the present case should be speculated. Karger-Kocsis et al.[28,29] has explained the formation of β-iPP in the shear-induced crystallization as follows: Shearing the melt of iPP generates row nuclei of α-modification (α-row nuclei). At the surface of these α-row nuclei, the α-to-β transition, termed as $\alpha\beta$ secondary nucleation, results in pointlike β-nuclei, which covered the surface of these α-row nuclei. Since the kinetic prerequisite of the $\alpha\beta$ transition is limited in the temperature range 100−140 °C, in which the growth rate of β-iPP crystals is much faster than that of the α-iPP crystals, the growth of the α-iPP crystals is, therefore, inhibited by the fast growing β-iPP crystals. As a result, cylindrites of β-iPP are formed at the sheared fiber/matrix interface. In our case, in considering the fact that the solid α-iPP fibers induce transcrystallization of iPP in its α-modification, while the molten or surface partially molten α-iPP fibers initiate the formation of β-iPP transcrystalline layers, it can be concluded that the melting of iPP fibers plays a very important role in the formation of β-iPP. From the fact that (i) the content of the β-iPP increases with increasing fiber introduction temperature and (ii), in particular, the formation of the β-iPP crystals is associated with the melting or at least surface partial melting of the iPP fiber, the β-iPP crystals may easily be thought to be also the result of shearing produced by fiber relaxation during melting. It is worth noting that in Figure 3b the relaxation bending of the fibers should create also some extent of shearing along the fiber axes. But this causes no detectable effect on the polymorphic behavior of the transcrystalline layers (compare parts a and b of Figure 3). The transcrystalline layers in both cases are composed of rich α-iPP crystals and a few of individual fan-shaped β-iPP crystals. This may imply that the tiny shearing produced by fiber relaxation is not sufficient enough to generate the β-iPP. Moreover, similar relaxation behavior is expected in the cases of Figures 5 and 6. The melting of iPP fibers at higher temperature is, however, not as effective in generating β-iPP as at lower temperatures (compare Figures 5 and 6). This helps to conclude that the tiny shearing produced by fiber relaxation is not the main reason for the formation of β-iPP.

Combining the facts that (i) the formation of β-iPP is associated with the melting or partial melting of the iPP fiber and (ii) the melting temperature of the iPP fibers (e.g., 173 and 178 °C) has a great effect on the polymorphic behavior of iPP, the origin of the formation of β-iPP may depend on the molten state of the iPP fibers. It was well documented that the domains remain active for crystallization when the α- or β-iPP samples are heated above the experimental melting points of iPP α- or β-modification, respectively.[14,26] The characteristics of the supermolecular structures formed after recrystallization of such samples have been explained by differentiating between "amorphous" and crystalline nuclei. To avoid the irritation[27] caused by the term "amorphous nuclei", the designation "prenuclei" of amorphous character was then used by Karger-Kocsis et al.[28] They have proven the existence of prenuclei. In the present case, the melting of iPP fibers at lower temperatures may originally result in the formation of amorphous domains composed of locally oriented, stretched macromolecular segments and chains. These stretched macromolecular segments or chains will crystallize easily during the cooling process. One may suggest that the crystallization process of the molten iPP fiber plays also a very important role in generating β-iPP. It may play the same role as the crystalline row nuclei generated by fiber pulling.

Conclusions

In conclusion, the homogeneity fiber/matrix composites of iPP have been successfully prepared by utilizing the fact that polymers crystallize only under supercoolings. The induced supermolecular structures of iPP by its homogeneity fibers as a function of fiber introduction temperature were studied by means of optical microscopy. The results show that the induced supermolecular structures of iPP at the fiber/matrix interfacial layer can be ascribed to the transcrystallization of iPP triggered by strong heterogeneous nucleation rather than the shearing produced by fiber introduction. It is further demonstrated that when the fibers were introduced at 138 °C, the interfacial transcrystalline iPP is composed of purely α-modification. As the fiber introduction

temperature increases, an increasing content of β-iPP surrounding the iPP fibers has been seen. Transcrystallization layers with mainly β-modification have been observed when T_{in} was set at 173 °C. This is related to the melting, or at least surface partial melting, of the iPP fibers. The formation of rich α-iPP transcrystallization layers at an even higher fiber introduction temperature, e.g., 178 °C, demonstrates that the melting state of the iPP fibers plays the leading role in generating the β-iPP. The molten iPP fibers at lower melting temperatures may act essentially as the "prenuclei" with amorphous character as depicted by Varga and Karger-Kocsis et al.

Acknowledgment. The financial support of The Chinese Academy of Sciences (Hundred Talents Program) and The National Natural Science Foundation of China (No. 20244003 and 50290090) are gratefully acknowledged.

References and Notes

(1) Turner-Jones, A.; Cobbold, A. J. *J. Polym. Sci.* **1968**, *B6*, 539.
(2) Bruckner, S.; Meille, S. V. *Nature (London)* **1989**, *340*, 455.
(3) Meille, S. V.; Bruckner, S.; Porzio, W. *Macromolecules* **1990**, *23*, 4114.
(4) Lotz, B.; Graff, S.; Straupe, C.; Wittmann, J. C. *Polymer* **1991**, *32*, 2902.
(5) Morrow, D. R.; Newman, B. A. *J. Appl. Phys.* **1968**, *39*, 4944.
(6) Lovinger, A. J.; Chua, J. O.; Gryte, C. C. *J. Polym. Sci., Polym. Phys. Ed.* **1977**, *15*, 641.
(7) Grubb, D. T.; Odell, J. A.; Keller, A. *J. Mater. Sci.* **1975**, *10*, 1510.
(8) Varga, J. *J. Therm. Anal.* **1989**, *35*, 1891.
(9) Varga, J. *J. Therm. Anal.* **1986**, *31*, 165.
(10) Devaux, E.; Chabert, B. *Polym. Commun.* **1991**, *32*, 464.
(11) Varga, J.; Karger-Kocsis, J. *Polym. Bull. (Berlin)* **1993**, *30*, 105.
(12) Varga, J.; Karger-Kocsis, J. *Polymer* **1995**, *36*, 4877.
(13) Varga, J.; Karger-Kocsis, J. *J. Mater. Sci., Lett.* **1994**, *13*, 1069.
(14) Varga, J. *J. Mater. Sci.* **1992**, *27*, 2557.
(15) Wang, C.; Liu, C.-R. *Polymer* **1999**, *40*, 289.
(16) Saujanya, C.; Radhakrishnan, S. *Polymer* **2001**, *42*, 4537.
(17) Wang, C.; Hwang, L. M. *J. Polym. Sci., Part B* **1996**, *34*, 1435.
(18) Folkes, M. J.; Hardwick, S. T. *J. Mater. Sci.* **1990**, *25*, 2598.
(19) Wang, C.; Liu, C. R. *Polymer* **1999**, *38*, 4715.
(20) Capiati, N. J.; Porter, R. S. *J. Mater. Sci.* **1975**, *10*, 1671.
(21) Mead, W. T.; Porter, R. S. *J. Appl. Polym. Sci.* **1978**, *22*, 3249.
(22) Loos, J.; Schimanski, T.; Hoffman, J.; Peijs, T.; Lemstra, P. J. *Polymer* **2001**, *42*, 3827.
(23) Ishida, H.; Bussi, P. *Macromolecules* **1991**, *24*, 3569.
(24) Stern, T.; Wachtel, E.; Marom, G. *J. Polym. Sci., Part B* **1997**, *35*, 2429.
(25) Stern, T.; Marom, G.; Wachtel, E. *Composites A* **1997**, *28*, 437.
(26) Varga, J.; Schulek-Tóth, F.; Ille, A. *Colloid Polym. Sci.* **1991**, *269*, 655.
(27) Fillon, B.; Thierry, A.; Wittannn, J. C.; Lotz, B. *J. Polym. Sci., Polym. Phys.* **1993**, *31*, 1407.
(28) Varga, J.; Karger-Kocsis, J. *J. Polym. Sci., Polym. Phys.* **1996**, *34*, 657.
(29) Wu, C.; Chen, M.; Karger-Kocsis, J. *Polymer* **1999**, *40*, 4195.

MA034062W